Biol Cybern (2007) 96:377–388
DOI 10.1007/s00422-007-0142-8

ORIGINAL PAPER

Biological Cybernetics

The role of the striatum in adaptation learning: a computational model

Moritz Grosse-Wentrup · Jose L. Contreras-Vidal

Received: 19 December 2005 / Accepted: 11 September 2006 / Published online: 16 March 2007

Abstract To investigate the functional role of the striatum in visuo-motor adaptation, we extend the DIRECT-model for visuo-motor reaching movements formulated by Bullock et al.(J Cogn Neurosci 5:408–435,1993) through two parallel loops, each modeling a distinct contribution of the cortico–cerebellar–thalamo–cortical and the cortico–striato–thalamo–cortical networks to visuo-motor adaptation. Based on evidence of Robertson and Miall(Neuroreport 10(5): 1029–1034, 1999), we implement the function of the cortico–cerebellar–thalamo–cortical loop as a module that gradually adapts to small changes in sensorimotor relationships. The cortico–striato–thalamo–cortical loop on the other hand is hypothesized to act as an adaptive search element, guessing new sensorimotor-transformations and reinforcing successful guesses while punishing unsuccessful ones. In a first step, we show that the model reproduces trajectories and error curves of healthy subjects in a two dimensional center-out reaching task with rotated screen cursor visual feedback. In a second step, we disable learning processes in the cortico–striato–thalamo–cortical loop to simulate subjects with Parkinson's disease (PD), and show that this leads to error curves typical of subjects with PD. We conclude that the results support our hypothesis, i.e., that the role of the cortico–striato–thalamo–cortical loop in visuo-motor adaptation is that of an adaptive search element.

M. Grosse-Wentrup (✉)
Institute of Automatic Control Engineering,
Technische Universiät München, 80290 München, Germany
e-mail: moritz@tum.de

J. L. Contreras-Vidal
Department of Kinesiology
and Graduate Programs in Bioengineering
and Neuroscience and Cognitive Science,
University of Maryland, College Park, MD 20742, USA
e-mail: pepeum@umd.edu

1 Introduction

Reaching movements to visual targets require the transformation of sensory signals about spatial target location and hand position into motor commands that move the hand in the direction of the target (Andersen and Buneo 2002; Burnod et al. 1999). Experimentally, visuo-motor transformations for reaching can be distorted by artificially rotating and/or scaling visual space via manipulation of the real-time visual feedback of hand movements displayed as a screen cursor on a computer monitor (computer-based distortions of hand–cursor relationships), or through the use of displacing or rotating prisms (Imamizu et al. 2000; Clower et al. 1996; Inoue et al. 2000). Under kinematic manipulations, practice is needed to acquire an internal model of the novel environment, i.e., a representation of the altered relationship between the screen cursor movement and the hand movement (Imamizu et al. 2000).

Functional imaging studies suggest that a widespread fronto-parieto-cerebellar network is involved in adapting the visuo-motor transformation to the new environment (Balslev et al. 2002; Contreras-Vidal and Kerick 2004; Inoue et al. 2000; Shadmehr and Holcomb 1997; Ghilardi et al. 2000; Imamizu et al. 2000). Surprisingly, the contribution of the striatum to the learning of novel environments has not received the same attention as frontal, parietal, and cerebellar structures (Inoue et al. 2000, 2001; Imamizu et al. 2000), even though clinical studies show that sensorimotor learning in response to

perturbed kinematic (Contreras-Vidal and Buch 2003; Stoffers et al. 2002; Teulings et al. 2002; Laforce Jr and Doyon 2002) and dynamic (Krebs et al. 2001) environments is impaired in diseases of the basal ganglia such as Parkinson's disease (PD).

In this article, we aim at elucidating the contribution of the striatum to adaptive visuo-motor behavior during the learning of novel kinematic environments through a computational model. Based on experimental evidence, we hypothesize that the role of the striatum in visuo-motor adaptation is that of an adaptive search element, guessing new sensorimotor transformations and rewarding successful while punishing unsuccessful ones, resulting in a coarse adaptation to the novel kinetic environment. This hypothesis is implemented in a computational model, and the performance of the model in a visuo-motor adaptation task is compared with data from healthy subjects and subjects with PD. As a first step, we show that the model reproduces movement trajectories and learning curves of healthy subjects in a center-out reaching task with rotated visual feedback. In a second step, we disable learning mechanisms in that part of the model representing the striatum to simulate dopamine depletion in subjects with PD, which results in error curves of the computational model that are characteristic of subjects with PD. We conclude that the evidence from the computational model supports our hypothesis, i.e., that the role of the striatum in visuo-motor adaptation learning is that of an adaptive search element.

The rest of this article is organized as follows. In Sect. 2.1 we introduce the motor equivalence problem for two-dimensional reaching tasks. In this study, the motor equivalence problem is solved using the DIRECT-model (Bullock et al. 1993), which is described in Sect. 2.2. For reaching movements under perturbed kinematic environments, introduced in Sect. 2.3, the DIRECT-model is extended by two side-loops, modeling the contribution of the cortico–cerebellar–thalamo–cortical and the cortico–striato–thalamo–cortical loop to visuo-motor adaptation. These extensions are presented in Sects. 2.4 and 2.5. In the results section we show simulation results of the extended model with and without learning processes enabled, and compare these to the behavior of healthy subjects and subjects with PD. The article concludes with a discussion of the results.

2 Methods

2.1 The motor equivalence problem

In order to successfully reach towards a target, the brain must compute muscle activations that rotate the joints in a way such that the end-effector, i.e., the hand, moves in direction of the desired target. In the present study, we only consider two-dimensional reaching movements in the horizontal plane, resulting in the workspace depicted in Fig. 1. Here, $\mathbf{x}_i \in \mathbb{R}^2, i = 1,\ldots,3$ describe the position of the arm joints, $\mathbf{x}_{\text{eff}}$ the position of the end effector, and $\mathbf{x}_{\text{T}}$ the target position. With $\mathbf{x}_1$ placed at the origin of the coordinate system, the position of the joints and the joint angles $\theta_i, i = 1,\ldots,3$ are related through

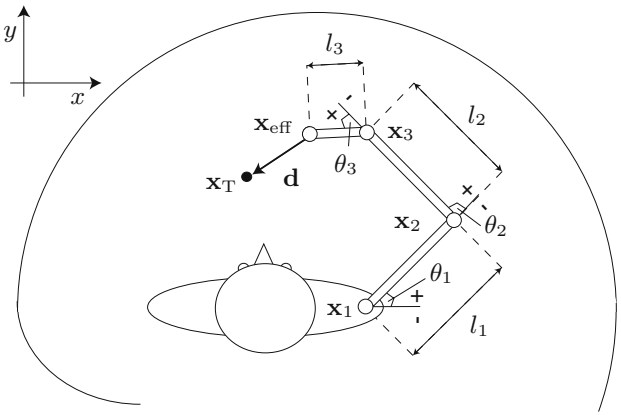

Fig. 1 Illustration of the workspace

$$\mathbf{x}_2 = \begin{pmatrix} l_1 \cdot \cos\theta_1 \\ l_1 \cdot \sin\theta_1 \end{pmatrix}, \tag{1}$$

$$\mathbf{x}_3 = \begin{pmatrix} l_1 \cdot \cos\theta_1 - l_2 \cdot \sin(\theta_1 + \theta_2) \\ l_1 \cdot \sin\theta_1 + l_2 \cdot \cos(\theta_1 + \theta_2) \end{pmatrix}, \tag{2}$$

$$\mathbf{x}_{\text{eff}} = \begin{pmatrix} l_1 \cdot \cos(\theta_1) - l_2 \cdot \sin(\theta_1 + \theta_2) - l_3 \cdot \cos\left(\frac{\pi}{2} - \sum_{i=1}^{3} \theta_i\right) \\ l_1 \cdot \sin(\theta_1) - l_2 \cdot \cos(\theta_1 + \theta_2) + l_3 \cdot \sin\left(\frac{\pi}{2} - \sum_{i=1}^{3} \theta_i\right) \end{pmatrix}. \tag{3}$$

To model physiological constraints, the joint angles are restricted to $\theta_1 \in \left\{-\frac{\pi}{2}, \pi\right\}, \theta_2 \in \{0, \pi\}$, and $\theta_3 \in \left\{-\frac{\pi}{2}, \frac{\pi}{2}\right\}$.

Linearization of (3) for a given joint configuration $\boldsymbol{\theta} = \{\theta_1, \theta_2, \theta_3\}^T$ results in a first order approximation of the change in position of the end effector due to a change in the joint angles

$$\dot{\mathbf{x}}_{\text{eff}} = J(\boldsymbol{\theta}) \cdot \dot{\boldsymbol{\theta}}, \tag{4}$$

with $J(\boldsymbol{\theta}) \in \mathbb{R}^{2\times 3}$ representing the Jacobian. The computation of a joint angle rotation that moves the end effector towards the target, however, requires the inverse of

the Jacobian. Since the rank of $J(\boldsymbol{\theta})$ can only be two, an infinite number of joint angle rotations exist that move the end-effector in the desired direction. Several approaches to this inverse problem of motor equivalence exist, ranging from introducing additional constraints to obtain a unique solution to neural network approaches (c.f., Bullock et al. 1993; Rosenbaum et al. 1993 and references therein).

2.2 The DIRECT-model

In this study, we adapt the DIRECT-model developed by Bullock et al. (1993) for solving the motor equivalence problem, which will be briefly presented in this section. The DIRECT-model was chosen, because it has been shown to produce reaching movement trajectories typical of human subjects, and because of its capability to account for some aspects of tool use and blind reaches. Since we are only interested in the kinematics of reaching movements, in our adaptation of the DIRECT-model we assume that the position of the end-effector $\mathbf{x}_{\text{eff}}$ and the target $\mathbf{x}_{\text{T}}$ as well as the direction vector $\mathbf{d}$ pointing from the end-effector to the target are already available to the model in a common reference frame, i.e., in cartesian coordinates with the origin at the position of $\mathbf{x}_1$.

Note that this implies that all information necessary for online error correction, i.e., information necessary for constant recomputation of motor commands that move the end-effector towards the target, are readily available to the model. Pathologies such as Huntington's disease, in which online error correction is disturbed (Smith and Shadmehr 2005), are thus outside the scope of this model.

Furthermore, we assume that the dynamics of the movements arising from mechanical properties of the arm and joints are controlled outside the model. All parameters used in the simulations are summarized in Table 1.

Based on the current joint configuration and direction vector, the DIRECT-model generates joint rotation commands r_i^{ag} and r_i^{an}, modeling the activation of agonist (ag) and antagonist (an) muscle groups rotating each joint $i = 1, \ldots, 3$, to move the effector towards the target. The joint angles, and thus the position of the joints, are then updated in each time step according to the difference equation

$$\theta_i[t+1] = \theta_i[t] + \epsilon \cdot \delta[t] \cdot (r_i^{\text{ag}} - r_i^{\text{an}}). \tag{5}$$

Here, ϵ determines the step size, and $\delta[t]$ ensures an approximately bell shaped velocity curve characteristic of reaching movements (reviewed in Bullock and Grossberg 1988) through the scaling function

Table 1 Parameters used in the model

Parameter	Value
l_1	16 cm
l_2	28 cm
l_3	28 cm
ϵ	0.05
α	0.9
β	0.002
γ	0.1
η	0.4
ξ	0.012
σ_ω	10.13
σ_ζ	0.04
λ_{pun}	0.15
λ_{rew}	0.15
ρ	0.2
υ	100
$\phi_{\text{threshold}}$	45°
τ_{IDE}	2

$$\delta[t] = \begin{cases} \dfrac{\alpha \cdot \left(2\frac{\|\mathbf{d}\|}{\|\mathbf{d}\|_{\text{initial}}}\right)^4}{\beta + \left(2\frac{\|\mathbf{d}\|}{\|\mathbf{d}\|_{\text{initial}}}\right)^4} + \gamma; & 1 \geq \frac{\|\mathbf{d}\|}{\|\mathbf{d}\|_{\text{initial}}} \geq 0.5 \\ \dfrac{\alpha \cdot \left(2\frac{\|\mathbf{d}\|}{\|\mathbf{d}\|_{\text{initial}}} - 2\right)^4}{\beta + \left(2\frac{\|\mathbf{d}\|}{\|\mathbf{d}\|_{\text{initial}}} - 2\right)^4} + \gamma; & 0.5 \geq \frac{\|\mathbf{d}\|}{\|\mathbf{d}\|_{\text{initial}}} \geq 0 \end{cases}, \tag{6}$$

with $\|\mathbf{d}_{\text{initial}}\|$ being the length of the direction vector upon start of a new reaching movement. It should be noted that the scaling function is not part of the original DIRECT-model, but was introduced here to obtain more realistic movement dynamics.

The activation of the agonist and antagonist muscle groups of each joint are determined by a neural network, calculating r_i^{ag} and r_i^{an} in two stages depending on the direction vector and the current joint configuration. The first stage encodes the current joint configuration and direction vector through $N = 30 \times 7 \times 7 \times 7 = 10,290$ cells, partitioning the direction vector space into 30 angular regions of the horizontal plane of 12° each, and the workspace of each joint into seven angular regions of approximately 51.4° each. Each cell corresponds maximally to a specific joint configuration and angle of the direction vector, determined by

$$C_n = 4 - \frac{1}{\pi}\|\angle\mathbf{d} - \angle\mathbf{d}_{\max_n}\| - \frac{1}{\pi}\sum_{i=1}^{3}\|\theta_i - \theta_{i,\max_n}\|. \tag{7}$$

Here, $\angle\mathbf{d}_{\max_n}$ and $\theta_{i,\max_n}$ describe the direction vector angle and joint configuration of maximal activation for each cell. These values are equally spaced between the cells, and their range is determined by the joint angle

restrictions of the arm model. The cell population $\mathbf{C} = \{C_1, \ldots, C_N\}$ thus encodes the current joint configuration and desired movement direction. To speed up computations, the activity of all except the seven most active cells is then set to zero, and the activity of the remaining cells is normalized to the most active cell.

Each cell C_n is connected to each of the three agonist and antagonist muscle groups with a specific weight $z_{n,r_i^{\text{ag/an}}}$, such that the activity of each muscle group $r_i^{\text{ag/an}}$ is determined by

$$r_i^{\text{ag/an}} = \sum_{n=1}^{N} C_n \cdot z_{n,r_i^{\text{ag/an}}}. \quad (8)$$

In order for the model to generate movements that move the end effector towards the target, the weights $z_{n,r_i^{\text{ag/an}}}, i = 1, \ldots, 3, n = 1, \ldots, N$ have to be trained such as to realize a solution of the Jacobian in (4). This is being done in a preliminary *motor-babbling*-phase, which will only briefly be outlined here (see Bullock et al. 1993 for details). At the start of the *motor-babbling*-phase all weights are set to zero, and a random joint configuration is generated. Then, random muscle activations $r_i^{\text{ag/an}}$ are generated for all joints, and the resulting movement of the end effector determined by (5) is observed. The vector pointing from the starting position of the end effector $\mathbf{x}_{\text{eff}}[t]$ to the updated position $\mathbf{x}_{\text{eff}}[t+1]$ is then considered as the direction vector $\mathbf{d}$, which conjointly with the joint configuration before the movement took place ($\boldsymbol{\theta}[t]$) is used to calculate the cell activation as given in (7). The weights are then updated according to

$$z_{n,r_i^{\text{ag/an}}}[t+1] = z_{n,r_i^{\text{ag/an}}}[t] + \eta \cdot C_n \cdot (r_i^{\text{ag/an}} - z_{n,r_i^{\text{ag/an}}}[t]) \quad (9)$$

with learning parameter η. By repeating this procedure with different random muscle activations and for different joint configurations, the neural network explores its workspace, and learns to map a joint configuration together with a desired movement direction to the muscle activations that move the end effector into the desired direction. It thereby approximates a solution of the Jacobian in (4).

2.3 Reaching under perturbed kinematic environments and visuo-motor adaptation

If the kinematic environment is perturbed, e.g., by rotating the (simulated) visual feedback about the position of the end effector $\mathbf{x}_{\text{eff}}$, the DIRECT-model will not be able to adapt it's input to output mapping to the new environment, resulting in movement trajectories

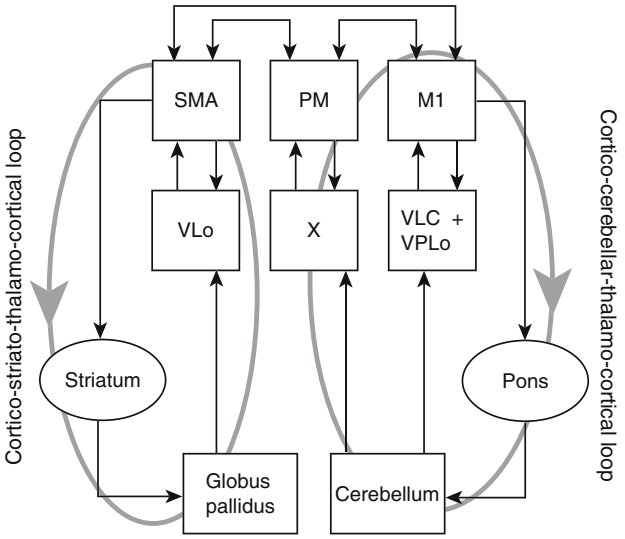

Fig. 2 Cortical and subcortical structures involved in motor learning (adapted with permission from Doyon et al. (2003))

circling the target. In principle, a new *motor-babbling*-phase could be initiated to learn the new Jacobian incorporating the feedback distortion, but this would require extensive training that does not take place in human subjects. Instead, it is well known that in case of kinematic perturbations human subjects quickly adapt to the new environment (Kagerer et al. 1997; Cunningham 1989; Roby-Brami and Burnod 1995). There is ample evidence (reviewed in Doyon et al. 2003) that this is due to the contributions of a cortico–cerebellar–thalamo–cortical and a cortico–striato–thalamo–cortical loop, acting in parallel to the structures mainly implicated in unperturbed reaching movements (see Fig. 2). The modeling of the contribution of these two loops to visuo-motor adaptation will be the subject of the next two sections.

In this study, we restrict perturbations of the kinematic environment to rotations of the visual feedback of the position of the end-effector, since this kind of transformation is well studied in both healthy human subjects and those with neurological disorders (Pine et al. 1996; Contreras-Vidal and Buch 2003). Thus, the only perturbation the model has to adapt to is a rotation of the vector $\mathbf{d}$, coding the direction of the intended movement. Although more complex transformations are possible, we expect that the basic principles of visuo-motor adaptation remain invariant. Due to the parallel organization, the adaptation mechanisms of the two loops are assumed to be independent of each other and of the mechanisms employed for normal reaching. Their respective contributions are then modelled as two correction terms applied to the vector coding the intended

direction movement,

$$\angle\tilde{\mathbf{d}} = \angle\mathbf{d} + \angle\mathbf{d}_{\text{Cerebellar}} + \angle\mathbf{d}_{\text{Striatal}}. \tag{10}$$

The direction vector $\angle\tilde{\mathbf{d}}$ then replaces $\angle\mathbf{d}$ in (7).

It should be pointed out that other mechanisms for combining the output of the two error correction loops could be considered as well. Nakahara et al. (2001) propose a time-variant weighted average of two parallel loops in visuomotor sequence learning, while Koerding and Wolpert (2004) present evidence for Bayesian integration in sensorimotor learning. Both approaches, however, would require another mechanism to determine the time-variant weighting of each of the two loops in the error correction process. The need for such an additional "coordinator"-structure is removed by simply adding the sum of the two error correction terms to the current movement direction as in (10). The consequences of this choice of combination for the dynamics of the adaptation process will be discussed in Sect. 2.6.

In the next two sections the specific contributions of each of the two loops to visuo-motor adaptation will be discussed, and it will be shown how the correction terms in (10) are being calculated.

2.4 The cortico–cerebellar–thalamo–cortical loop

Based on the observation that adaptation to gradual visual distortions is inhibited by inactivation of the dentate nucleus, it has been suggested that visuo-motor adaptation to gradual distortions may depend on adaptive cerebellar mechanisms for gradual acquisition of a new internal model (Robertson and Miall 1999). This interpretation of the role of the cerebellum in visuomotor adaptation is further supported by Doya (2000), reviewing evidence for a specialization of the cerebellum for error-based learning. In this view, the detection of small deviations of the movement direction from the desired direction are transformed into a correction term, that is used conjointly with the original internal representation to ensure movement of the end effector in direction of the target.

Following these considerations, we model the cortico–cerebellar–thalamo–cortical loop through a system supervising the deviation of the real from the intended movement direction, and adding a correction term to the intended movement direction. This correction term depends on the direction of the intended movement, i.e., each distinct movement direction has an associated correction term, and is adapted according to the evaluation of the current movement direction error. The coding of the current desired movement direction is performed analogous to (7), with $M = 12$ cells partitioning the workspace of the direction vector into angular regions of 30° each,

$$C^m_{\text{Cerebellar}} = 1 - \frac{1}{\pi} \cdot \|\angle\mathbf{d} - \angle\mathbf{d}_{\max_m}\|, \quad m = 1, \ldots, M. \tag{11}$$

Here, the activity of all except the most active cell are set to zero, and the activity of the remaining cell is set to one, such that (11) acts as an indicator function for the angular region of the current direction vector. The correction term applied to the direction vector is then calculated by

$$\angle\mathbf{d}_{\text{Cerebellar}} = \sum_{m=0}^{M} C^m_{\text{Cerebellar}} \cdot w_m. \tag{12}$$

The weights of this network w_m, $m = 1, \ldots, M$, which are initially set to zero, are updated according to the difference equation

$$w_m[t+1] = w_m[t] - \xi \cdot \varphi[t] \cdot C^m_{\text{Cerebellar}}. \tag{13}$$

Here, ξ is a learning parameter, and

$$\varphi[t] = \angle\{\mathbf{x}_{\text{eff}}[t] - \mathbf{x}_{\text{eff}}[t-1]\} - \angle\mathbf{d}[t-1]$$

is the error term, describing the angle between the desired movement direction and the actual movement direction.

The cortico–cerebellar–thalamo–cortical loop of the model thus gradually adapts to a rotation of the visual feedback of the end effector position.

2.5 The cortico–striato–thalamo–cortical loop

If the visual feedback about the position of the end effector is suddenly rotated by more than approximately 40°, human subjects do not employ gradual adaptation mechanisms anymore but rather start exploring the new environment in a different way (Kagerer et al. 1997; Buch et al. 2003). Based on observations of the trajectories of adaptation to sudden rotations of healthy subjects (see for example, Fig. 4), we hypothesize that this adaptation mechanism is that of an adaptive search mechanism, guessing new transformations and rewarding successful while punishing unsuccessful transformations. Moreover, as it appears that this type of adaptation is employed only in early phases of the adaptation to a sudden cursor rotation (i.e., when the angular error between the desired and actual direction of movement is

larger than some threshold) the mechanism is assumed to be only active until a stable guess of the transformation has been found that keeps the error below the threshold necessary to engage the search mechanism.

This type of adaptation mechanism is in agreement with the hypothesized role of the cortico–striato–thalamo–cortical loop in visuo-motor adaptation. There is evidence presented in Krebs et al. (2001) and Contreras-Vidal and Buch (2003) that adaptation to a novel task environment involves the basal ganglia. Furthermore, Krebs et al. (1998) as well as Seidler et al. (2006) have shown that the basal ganglia are only activated during early stages of the adaptation process. In this view, rotations of the visual feedback of less than 40° are not considered as a novel task environment, and thus do not recruit the cortico–striato–thalamo-cortical loop. If, however, the visual feedback is rotated by more than 40° a novel task environment is detected, and the cortico–striato-thalamo-cortical loop is activated to find a coarse adaptation to this new environment. As soon as an adaptation has been obtained that keeps the angular movement error below 40°, i.e., in later stages of the adaptation process, the cortico–striato–thalamo–cortical loop is disengaged again. We thus hypothesize that the proposed adaptive search mechanism is executed within the cortico–striato–thalamo–cortical loop. We furthermore would like to point out that this assumption is also in agreement with evidence reviewed by Doya (2000) that the basal ganglia are specialized for reward-based learning.

The adaptive search mechanism, assumed to model the functional role of the cortico–striato–thalamo–cortical loop, is thus implemented with two cell layers in the following way. Analogous to Eqs. (7) and (11), the current intended movement direction is coded in the first layer by $L = 12$ cells, again partitioning the workspace into 12 angular regions of 30° each,

$$C^l_{\text{Striatum}} = 1 - \frac{1}{\pi} \cdot \| \angle \mathbf{d} - \angle \mathbf{d}_{\max_l} \|, \quad l = 1, \ldots, L. \quad (14)$$

As previously, $\angle \mathbf{d}_{\max_l}, l = 1, \ldots, L$ code the direction for which each cell l is most active, the most active cell is normalized, and the activity of all other cells is set to zero. The second layer, however, deviates significantly from the second layer of the cortico–cerebellar–thalamo–cortical loop. It consists of $L = 12$ groups of $K = 30$ cells for each of the L cells in the first layer. In this second layer, each cell represents a rotational transformation in steps of 12°, such that the first cell of each group represents a rotational bias of 0°, the second cell a bias of 12°, etc. The weights between the first and the second layer of the module are initialized as

$$w_{l,k} = \begin{cases} \mathrm{e}^{\frac{-k^2}{\sigma_w^2}} & ; \quad k = 1, \ldots, \frac{K}{2} \\ \mathrm{e}^{\frac{-(k-K)^2}{\sigma_w^2}} & ; \quad k = \frac{K}{2}, \ldots, K \end{cases} ; \; l = 1, \ldots, L, \quad (15)$$

such that the weights $w_{l,K}$ between the cells coding the movement direction (l) to those coding for a rotational bias of 0° ($k = K$) are initially the strongest. The activities of the cells in the second layer are then calculated as

$$C^{l,k}_{\text{Striatum}} = C^l_{\text{Striatum}} \cdot w_{l,k} + \zeta, \quad (16)$$

with ζ drawn from a Gaussian distribution with zero mean and variance σ^2_ζ. The actual rotational correction term in (10) is then determined in a winner-take-all (WTA) fashion as

$$\angle \mathbf{d}_{\text{Striatum}} = \frac{2\pi}{K} \cdot \tilde{k} \quad (17)$$

with

$$\tilde{k} = \max_{k=1\ldots K} \left\{ \sum_{l=1}^{L} C^{l,k}_{\text{Striatum}} \right\}. \quad (18)$$

In this way, for each angular region of the intended movement direction, a different rotational correction term is added to the direction vector. Since this correction term is partially determined by the random variable ζ in (16), the weights $w_{l,k}$ encode the probability that a certain rotational correction is employed. The stronger $w_{l,k}$, the more likely it is that the rotational bias coded by cell $C^{l,k}_{\text{Striatum}}$ is being chosen as the actual bias in each time step.

To be able to adjust to new transformations, the model has to observe its performance, and adapt its weights that determined the rotational correction term of the previous time step if the intended and actual movement direction differed by more than a threshold angle $\phi_{\text{threshold}}$. The adaptation is done by punishing rotational corrections that did not lead to a movement direction error $\phi \leq \phi_{\text{threshold}}$, and rewarding transformations that kept ϕ below the threshold. Thus,

$$w_{l,k}[t+1] = w_{l,k}[t] + \begin{cases} -\lambda_{\text{pun}} \cdot C^l_{\text{Striatum}} \cdot \left(1 - \mathrm{e}^{-\rho \cdot w_{l,k}[t]}\right), & \phi > \phi_{\text{threshold}} \\ \lambda_{\text{rew}} \cdot C^l_{\text{Striatum}} \cdot \mathrm{e}^{-\rho \cdot w_{l,k}[t]}, & \phi \leq \phi_{\text{threshold}} \end{cases} \quad (19)$$

Note that due to partitioning of the workspace into angular regions of 30° each a slightly higher threshold angle of 45° was chosen. To model a transfer of

transformations applied to one angular region of the direction vector to other regions as observed in human subjects (Krakauer et al. 2000), all weights are furthermore updated according to the rule

$$w_{l,k} = \frac{1}{\upsilon}\left((\upsilon - 1)\cdot w_{l,k} + \frac{1}{L}\cdot\sum_{l=1}^{L} w_{l,k}\right), \quad k = 1,\ldots,K. \tag{20}$$

In summary, the proposed model of the cortico–striato–thalamo–cortical loop behaves in the following way. In each time step, a certain rotational correction term as determined by (16)–(18) is applied to the movement direction. For the movement direction indicated by l, the value of this correction term is probabilistic, with the probability of a rotational correction of $k \cdot 12°$ defined by the weight $w_{l,k}$. Initially, the values of the weights are chosen such that a rotational correction term of zero degrees has the highest probability, and all other transformations are unlikely to occur. If the model is performing reaching movements under unperturbed kinematics, the difference between the intended and the actual movement direction will be small, resulting in the correct rotational guess of zero degrees being further rewarded in (19). Equation (20) however ensures that no weight grows without bounds. If at a certain point in time the visual feedback of the position of the end effector is rotated by more than $\phi_{\text{threshold}}$, a rotational guess of zero degrees will lead to a difference between the intended and the actual movement direction of more than $\phi_{\text{threshold}}$. Accordingly, in (19) the weights coding the probability of a rotational correction of zero degrees will be reduced. This procedure will be repeated several times, until the weights have become small enough that ζ in (16) mainly determines the next rotational correction term. At this point, the model commences its adaptive search mechanism. If a certain, now mainly randomly determined, rotational guess leads to a movement direction error below the threshold angle, the respective weight $w_{l,k}$ between the cell C^{l}_{Striatum} coding the current angular region of the direction vector and the cell $C^{l,k}_{\text{Striatum}}$ representing the successful rotational transformation will be strengthened in (19). This raises the probability of this specific successful rotational correction term being chosen again in a subsequent step, thereby leading to a convergence of the rotational correction term to a value that keeps the movement direction error below the threshold angle. As a result of this self-enforcing strategy, the value of the weight coding a correct rotational correction will become large in comparison to ζ, such that the applied rotational correction term in (16) will again be mainly determined by the weights regardless of the value of ζ. The adaptive search mechanism thereby disengages itself as soon as a crude adaptation to the new perturbed kinematic environment has been achieved.

2.6 Dynamics of the adaptation process

The dynamics of the adaptation of the model to a rotation of the visual feedback are determined by the dynamics of each of the two adaptation loops, as well as by the combination of the error correction term provided by each loop in (10). If the visual feedback is rotated by less than $\phi_{\text{threshold}}$, the adaptive search element of the cortico–striato–thalamo–cortical loop is not engaged. The gradual adaptation of the cortico–cerebellar–thalamo–cortical loop however will slowly adapt to the rotation, with the error correction term $\angle\mathbf{d}_{\text{Cerebellar}}$ in (12) asymptotically approaching the actual rotation. The speed of the convergence of this error-based learning is determined by the value of ξ in (13), which was experimentally chosen to reproduce the time course of the adaptation of human subjects to small rotations of the visual feedback. If the visual feedback is rotated by more than $\phi_{\text{threshold}}$, the cortico–striato–thalamo–cortical loop is engaged as well. Due to the reward-based type of learning (19), the error correction of this loop acts on a much faster time scale than that of the cortico–cerebellar–thalamo–cortical loop. The cortico–striato–thalamo–cortical loop will enforce guesses of the rotational error that keep the movement error below $\phi_{\text{threshold}}$, thereby quickly settling on a value of $\angle\mathbf{d}_{\text{Striatum}}$ that approximates the actual rotation of the visual feedback with an error of less than $\phi_{\text{threshold}}$. At this point the cortico–striato–thalamo–cortical loop automatically disengages itself, and the remaining error of the visual rotation is asymptotically driven to zero by the cortico–cerebellar–thalamo–cortical loop in the same way as for rotations of the visual field by less than $\phi_{\text{threshold}}$. It should be noted that the error correction terms supplied by each of the two loops in (10) are complimentary: a correction term supplied by one of the two loops decreases the overall movement error, such that the other loop only approximates the remaining error. In this way, no overcompensation can take place. The different time scales of the two error correction loops furthermore ensure that no oscillations occur.

3 Results

To simulate several subjects, five different instantiations of the DIRECT-model were trained through motor-babbling, i.e., a certain amount of simultaneous exposure

to patterned proprioceptive and visual stimulation under conditions of self-produced movement (see Sect. 2 and Bullock et al. 1993; Guigon and Baraduc 2002).

The performance of the model was then tested in a center-out reaching task to targets located in the corners of a quadrangle as shown in Fig. 3. This reaching experiment consisted of 11 blocks of 40 movements each, with ten movements per target within each block. The target order within each block was pseudo-randomized. During the first block, no rotation of the visual feedback of the position of the end effector was applied (pre-exposure condition). With the start of the second block however, the visual feedback was rotated counter-clockwise by 90° (exposure condition). This rotation was held constant for all until the last block, in which the rotation of the visual feedback was removed (post-exposure condition).

The resulting trajectories are shown in Fig. 4, along with data of human subjects performing the same task, adapted from Buch et al. (2003). The thick lines represent the mean trajectories of five human healthy young subjects (age 21 ± 2.7 years) for the measured data, and the mean trajectories of five instantiations of the model for the simulated data within each condition. The shaded areas show the standard deviation of the trajectories. Furthermore, the trajectories of ten single trials were plotted for each condition.

In order to compare the performance of the model with the measured data quantitatively, we furthermore calculated the RMSE of each movement, defined as

$$\mathrm{RMSE} = \sqrt{\frac{1}{T}\sum_{t=1}^{T}(x[t]-\hat{x}[t])^2 + (y[t]-\hat{y}[t])^2}, \qquad (21)$$

with $x[t], y[t], t = 1, \ldots, T$, representing the points of each simulated trajectory in cm, and $\hat{x}[t], \hat{y}[t]$ representing the points of a straight line leading from the center to the target recorded at the same sampling rate. Additionally, we calculated the initial direction error (IDE) of each movement, defined as

$$\mathrm{IDE} = \angle\{\mathbf{x}_{\mathrm{eff}}[t_0+\tau_{\mathrm{IDE}}] - \mathbf{x}_{\mathrm{eff}}[t_0]\} - \angle\{\mathbf{d}_T\}, \qquad (22)$$

with t_0 the initial time of each new reaching movement, and $\mathbf{d}_T$ the vector pointing from the center to the desired target.

As can be seen in Fig. 4a, in the pre-exposure condition the human subjects as well as the model produce smooth trajectories from the starting point to each target with little variance in the movements. In this condition, due to the small deviations of the intended and real movement direction, the two side-loops of the model, although active, hardly have any influence on the resulting movements. We thus conclude that our adaptation of the DIRECT-model reproduces the trajectories typical of human subjects in reaching movements without perturbations of the kinematic environment.

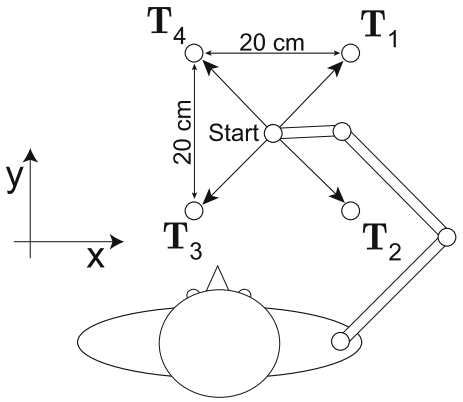

Fig. 3 Illustration of the center-out reaching task

For the early exposure (first block after onset of the visual rotation), spiral like trajectories can be observed for the human subjects as well as for the simulated data. Furthermore, it can be observed that the adaptive search mechanism is engaged in the model, resulting in somewhat erratic single trajectories with frequent changes of movement direction, which can also be seen in the measured trajectories. This also manifests itself in a high RMSE and IDE score for both simulated and measured data (Fig. 5).

In the late exposure stage, i.e., in the last block in which the visual rotation was still applied, the trajectories have become rather smooth again, with only a slight spiral like shape remaining. Thus, the human subjects as well as the model have adapted successfully to the rotation of the visual feedback, also resulting in small RMSE and IDE scores. As can be seen in the evolution of the RMSE and IDE scores, this adaptation takes place in two stages - an initial fast and coarse adaptation, followed by a slower gradual adaptation. In the simulated data the fast initial adaptation is due to the model of the cortico–striatal–thalamo–cortical loop, which disengages itself after a coarse adaptation has been achieved. At this point, the slope of the error curves is determined by the model of the cortico–cerebellar–thalamo–cortical loop, resulting in a slow but very precise adaptation to the rotation of the visual feedback.

If the visual rotation is removed again (post-exposure condition), the after-effects manifest themselves as spiral-like trajectories in opposite direction of those characteristic of the early exposure stage, and a high RMSE and IDE, with the IDE having opposite sign in comparison to the early-exposure stage.

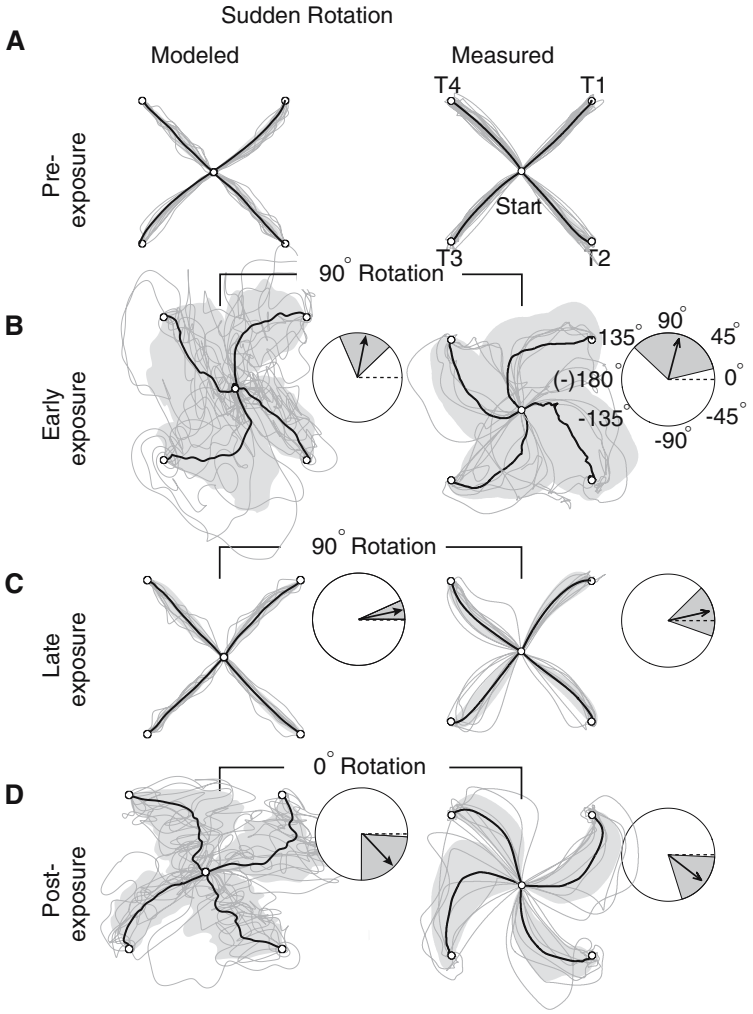

Fig. 4 Trajectories produced in the center-out reaching task under unperturbed and perturbed visual feedback. In these figures, the first two traces per target direction for each condition and each subject have been overlaid to show typical movement paths at different stages of learning (e.g., sharp reversals, spirals, loops, etc). Insets: The dark vectors represent mean normalized shifts of the initial movement direction, collapsed across targets, from pre-exposure to early- (**b**), late- (**c**), and post-exposure trials (**d**), respectively. The mean initial direction of movement at pre-exposure (represented as a *broken dark line*) is set to 0°. Adapted with permission from Fig. 2 of Buch et al. (2003).

In summary, the model reproduces the trajectories of human subjects in the center-out reaching task with rotated visual feedback in all stages of the adaptation process. Also, the evolution of the RMSE and IDE scores during the different stages of the adaptation agree rather well. However, the RMSE and IDE scores of the simulated data are initially higher than in the measured data. This is also apparent in the observed trajectories of the early-exposure and post-exposure stages, with the model performing more erratic movements than can be observed in the human subjects. This is most likely due to the following reason. Human subjects often reduce the speed of their movements if they notice a large error in their movement direction, then try out small movements in several directions, and only increase their speed again if they are moving closer to the target. Modeling this strategy would require a more sophisticated velocity curve $\delta[t]$ in (6), and would result in less erratic movement in early stages of the adaptation, thereby smoothing the trajectories and leading to a lower RMSE and IDE scores. This behavior however is not central to the functional role of the cortico–striato–thalamo–cortical loop, and was thus not further considered here.

In spite of these quantitative differences, the model reproduces the shape of the trajectories accurately in all stages of the adaptation process, and furthermore displays similar shapes of the RMSE and IDE curves to those of human subjects. While we do not claim that our model captures all mechanisms of visuo-motor adaptation, we conclude that the model is sufficiently accurate to be used in an investigation of the functional role of the cortico–striato–thalamo–cortical loop.

To further investigate the functional role of the cortico–striato–thalamo–cortical loop, we compared the performance of the model with that of subjects with PD. For this purpose, we deactivated learning processes in the model of the cortico–striato–thalamo–cortical loop by setting $\lambda_{\text{pun}} = \lambda_{\text{rew}} = 0$ in (19). This models the neurodegeneration of dopaminergic nigrostriatal neurons in PD (Fahn and Sulzer 2004; Kish et al. 1988), since phasic midbrain dopamine neuron activity is critically involved in reinforcement learning mechanisms

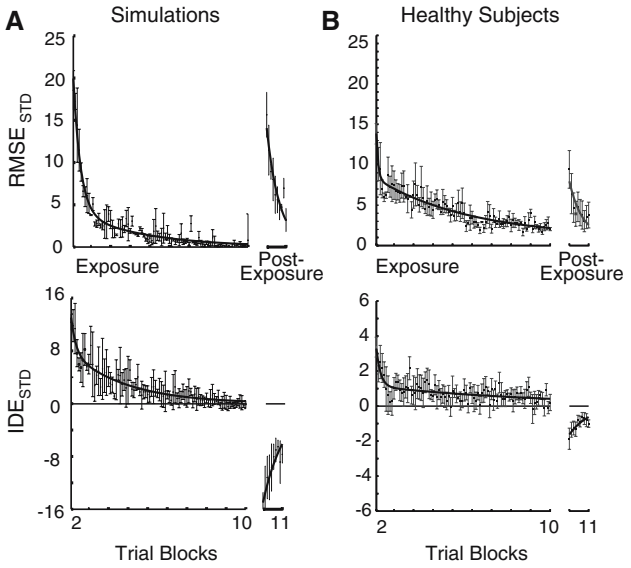

Fig. 5 Standardized RMSE and IDE scores of measured and simulated trajectories. For better visualization the data has been fitted with double exponential functions. Note that both the experimental and simulated error scores are standardized with respect to the pre-exposure (standard mapping) condition. Experimental data adapted with permission from Fig. 3 of Buch et al. (2003)

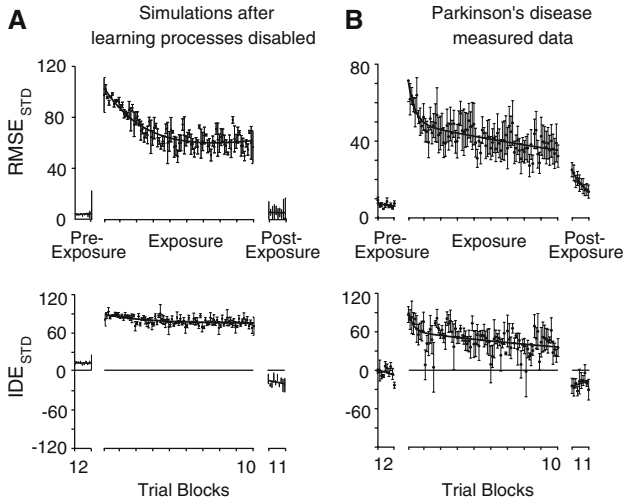

Fig. 6 RMSE and IDE scores of simulations without learning processes and patients with PD. Adapted with permission from Fig. 3 of Contreras-Vidal and Buch (2003)

(Fahn and Schultz et al. 1997). Importantly, as long as the movement direction error is small, i.e., without or with only small simulated visual rotations, this change has no effect on the behavior of the model, i.e., the performance of the selected movement is not compromised. Once the movement direction error exceeds the threshold angle, and the adaptive search mechanism is engaged, the model displays a different behavior than with an intact model of the cortico–striatal–thalamo–cortical loop. While in both cases the adaptive search mechanism starts to explore the space of possible rotations, the adaptive search mechanism with learning disabled can not reinforce good or punish bad guesses of the visual rotation angle. Consequently, the model does not stop guessing transformations, resulting in continuous erratic movements that usually are only observed during early stages of the adaptation. The model thus does not find a coarse adaptation to the new environment. This is reflected in the resulting RMSE score (Fig. 6a), that, although showing an initial decrease, converges to a rather large value. This also holds for the IDE score, that converges to a value only slightly below the 90° rotation of the visual feedback.

Comparing these results with experimental data gathered from subjects with PD reveals similar observations (Fig. 6b, adapted from Contreras-Vidal and Buch 2003). In agreement with the simulated data, the adaptation to the visual rotation is only very crude. After an initially fast decrease in RMSE and IDE, the scores settle on rather large values, with only a slight linear decrease still remaining in later stages of the adaptation process. With learning processes disabled in the adaptive search mechanism, the model thus qualitatively reproduces the behavior of subjects with PD.

4 Discussion

4.1 Biological relevance

Behavioral, inactivation, and neuroimaging experiments support the view of separate parallel networks for adaptation to gradual and sudden kinematic distortions.

Behaviorally speaking, the initial rapid change and the later gradual reduction in the mean error scores (e.g., RMSE or IDE) during exposure to a kinematic distortion in several studies (Krakauer et al. 2004; Buch et al. 2003; Kagerer et al. 1997; Contreras-Vidal and Buch 2003) suggest that there are two processes operating during the course of adaptation to kinematic distortions (Krakauer et al. 2000). The rapid exponential portion of the learning curve may be attributed to the initial acquisition and/or selection of a behaviorally appropriate internal model, whereas the latter almost linear component may involve processes that progressively fine-tune the selected internal model to the specific task conditions.

Adaptation to visual distortions introduced gradually (Kagerer et al. 1997; Robertson and Miall 1999; Ingram et al. 2000) may depend on cerebellar error-correction mechanisms for gradual acquisition of a new

internal model. Robertson and Miall (1999) have shown that adaptation to gradual visual distortions is blocked by inactivation of the dentate nucleus, whereas sudden adaptation is spared in non-human primates. This suggested that the lateral cerebellum may be implicated selectively in adaptation to gradual as opposed to sudden kinematic distortions. In the case of gradual distortions, the original internal model engaged prior to a gradual distortion can still be employed to help develop the new internal model of the task. Thus, subjects can utilize information regarding the original internal model together with memorization of trial-to-trial error correction signals to be used at the onset of the next movement (Roby-Brami and Burnod 1995). However, in the case of sudden rotations, the awareness or detection of large, explicit errors may engage different adaptation mechanisms that involve the use of various types of corrective actions. Nevertheless, as adaptation progresses and errors are reduced through practice, cerebellar structures may be recruited to fine-tuning the internal model of the sensorimotor transformation.

4.2 Neuroimaging studies of adaptation learning

The involvement of cerebellar structures in kinematic adaptation in humans has been clearly demonstrated by the elegant study of Imamizu et al. (2000), who showed bilateral focal activation in the lateral cerebellar hemispheres after a period of adaptation to a screen cursor rotation in a tracking task. Importantly, this error was not related to performance level as the mean error scores were equalized across the last baseline and adaptation blocks. However, neuroimaging studies of adaptation learning have produced conflicting results regarding the role of the basal ganglia on adaptation to kinematic perturbations, despite reports of deficits in patients with Parkinsons disease (Contreras-Vidal and Buch 2003). While in some cases, the authors were not looking at the whole brain (e.g., Imamizu et al. 2000), other neuroimaging studies using whole head scanning have not shown basal ganglia involvement in adaptation to screen cursor rotations (e.g., Ghilardi et al. 2000; Krakauer et al. 2004), or have shown early involvement during adaptation to gain changes only (Krakauer et al. 2004). However, the studies have used PET imaging, which averages signal over a relatively long time period and which have limited spatial resolution. Thus, these studies may have missed early, focal basal ganglia activation during adaptation to rotational perturbations. Interestingly, a recent fMRI study involving a large number of subjects ($N = 26$) showed bilateral basal ganglia activation very early in the rotational adaptation process only (Seidler et al. 2006). Thus, some issues of statistical power may also help to explain the lack of statistically significant activation of the basal ganglia in sensorimotor adaptation in previous imaging studies.

4.3 Conclusions

In this article, we adapted the DIRECT-model of Bullock et al. (1993) to perform two dimensional reaching movements in a center-out reaching task. To model the functional roles of the cortico–cerebellar–thalamo–cortical and the cortico–striato–thalamo–cortical loops in visuo-motor adaptation, we augmented the model by two side loops, generating correction terms for the planned movement direction of the DIRECT-model.

Based on the results of other behavioral as well as imaging studies, we modeled the function of the cortico–cerebellar–thalamo–cortical loop as that of a gradual adaptation mechanism. The function of the cortico–striato–thalamo–cortical loop on the other hand was hypothesized to be that of an adaptive search mechanism. These two models were implemented as side parallel loops, generating correction terms for the movement direction of the DIRECT-model.

The complete model was tested in a center-out reaching task with rotated visual feedback, and the performance was compared to that of human subjects. While quantitative differences were observed, the qualitative behavior of the model agreed well with the experimental data in all stages of the adaptation process. To test our hypothesis, we simulated subjects with PD by disabling learning mechanisms in the cortico–striato–thalamo–cortical loop of the model. This resulted in RMSE and IDE scores in the different stages of the adaptation process that qualitatively agreed with experimental data from human subjects with PD. We thus conclude that our results support the hypothesis that the functional role of the cortico–striato–thalamo–cortical loop in visuo-motor adaptation is that of an adaptive search mechanism, searching and exploring different sensorimotor transformations until a crude adaptation to the new environment has been achieved.

Acknowledgments Contreras-Vidal's work was supported by DARPA BICA Award FA87500520272.

References

Andersen RA, Buneo CA (2002) Intentional maps in posterior parietal cortex. Annu Rev Neurosci 25:189–220

Balslev D, Nielsen FA, Frutiger SA, Sidtis JJ, Christiansen TB, Svarer C, Strother SC, Rottenberg DA, Hansen LK, Paulson OB, Law I (2002) Cluster analysis of activity-time series in motor learning. Hum Brain Map 15(3):135–145

Buch ER, Young S, Contreras-Vidal JL (2003) Visuomotor adaptation in normal aging. Learn Memory 10(1):55–63

Bullock D, Grossberg S (1988) Neural dynamics of planned arm movements: emergent invariants and speed-accuracy properties during trajectory formation. Psychol Rev 95:49–90

Bullock D, Grossberg S, Guenther FH (1993) A self-organizing neural model of motor equivalent reaching and tool use by a multijoint arm J Cogn Neurosci 5:408–435

Burnod Y, Baraduc A, Battaglia-Mayer A, Guigon E, Koechlin E, Ferraina S, Lacquaniti F, Caminiti R (1999) Parieto-frontal coding of reaching: an integrated framework. Exp Brain Res 129:325–346

Clower DM, Hoffman JM, Votaw JR, Faber TL, Woods RP, Alexander GE (1996) Role of posterior parietal cortex in the recalibration of visually guided reaching. Nature 383:618–621

Contreras-Vidal JL, Buch ER (2003) Effects of Parkinson's disease on visuo-motor adaptation. Exp Brain Res 150:25–32

Contreras-Vidal JL, Kerick SE (2004) Independent component analysis of dynamic brain responses during visuomotor adaptation. Neuroimage 21(3):936–945

Cunningham HA (1989) Aiming error under transformed spatial mappings suggests a structure for visual-motor maps. J Exp Psychol Hum Percept Perform 15:493–506

Doya K (2000) Complementary roles of basal ganglia and cerebellum in learning and motor control. Curr Opin Neurobiol 10:732–739

Doyon J, Penhune V, Ungerleider LG(2003) Distinct contribution of the cortico-striatal and cortico-cerebellar systems to motor skill learning. Neuropsychologica 41(3):252–262

Fahn S, Sulzer D (2004) Neurodegeneration and neuroprotection in Parkinson disease. NeuroRx 1(1):139–154

Ghilardi MF, Ghez C, Dhawan V, Moeller J, Mentis M, Nakamura T, Antonini A, Eidelberg D(2000) Patterns of regional brain activation associated with different forms of motor learning. Brain Res 871:127–145

Guigon E, Baraduc P (2002) A neural model of perceptual-motor alignment. J Cogn Neurosci 14:538–549

Imamizu H, Miyauchi S, Tamada T, Sasaki Y, Takino R, Putz B, Yoshioka T, Kawato M(2000) Human cerebellar activity reflecting an acquired internal model of a new tool. Nature 403:192–195

Ingram HA, van Donkelaar P, Cole J, Vercher JL, Gauthier GM, Miall RC(2000) The role of proprioception and attention in a visuomotor adaptation task. Exp Brain Res 132:114–126

Inoue K, Kawashima R, Satoh K, Kinomura S, Sugiura M, Goto R, Ito M, Fukuda H (2000) A PET study of visuomotor learning under optical rotation. Neuroimage 11:505–516

Inoue K,Kawashima R, Sugiura M, Ogawa A, Schormann T, Zilles K, Fukuda F(2001) Activation in the ipsilateral posterior parietal cortex during tool use: a PET study. Neuroimage 14:1469–1475

Kagerer FA, Contreras-Vidal Jl, Stelmach GE (1997) Adaptation to gradual as compared with sudden visuo-motor distortions. Exp Brain Res 115:557–561

Kish SJ, Shannak K, Hornykiewicz O (1988) Uneven pattern of dopamine loss in the striatum of patients with idiopathic Parkinson's disease, pathophysiologic and clinical implications. New England J Med 318(14):876–880

Koerding K, Wolpert DM (2004) Bayesian integration in sensorimotor learning. Nature 427:244–247

Krakauer JW, Ghilardi MF, Mentis M, Barnes A, Veytsman M, Eidelberg D, Ghez C (2004) Differential cortical and subcortical activations in learning rotations and gains for reaching: a PET study. J Neurophysiol 91:924–933

Krakauer JW, Pine ZM, Ghilardi MF, Ghez C (2000) Learning of visuomotor transformations for vectorial planning of reaching trajectories. J Neurosci 20(23):8916–8924

Krebs HI, Brashers-Krug T, Rauch SL, Savage CR, Hogan N, Rubin RH, Fischman AJ, Alpert NM (1998) Robot-aided functional imaging: application to a motor learning study. Hum Brain Map 6:59–72

Krebs HI, Hogan N, Heing W, Adamovich SV, Poizner H (2001) Procedural motor learning in Parkinson's disease. Exp Brain Res 141:425–437

Laforce Jr R, Doyon J (2002) Differential role for the striatum and cerebellum in response to novel movements using a motor learning paradigm. Neuropsychologia 40:512–517

Nakahara H,Doya K, Hiskosaka O (2001) Parallel cortico-basal ganglia mechanisms for acquisition and execution of visuomotor sequences - a computational approach. J Cogn Neurosci 13(5):626–647

Pine ZM, Krakauer J, Gordon J, Ghez C (1996) Learning of scaling factors and reference axes for reaching movements. Neuroreport 7:2357–2361

Robertson EM, Miall RC (1999) Visuomotor adaptation during inactivation of the dentate nucleus. Neuroreport 10(5):1029–1034

Roby-Brami A, Burnod Y (1995) Learning a new visuomotor transformation: error correction and generalization. Cogni Brain Res 2:229–242

Rosenbaum DA,Engelbrecht SE, Bushe MM,Loukopoulos LD (1993) A model for reaching control. Acta Psychologica 82(1–3):237–250

Schultz W,Dayan P, Montague PR (1997) A neural substrate of prediction and reward. Science 275:1593–1599

Seidler RD, Noll DC, Chintalapati P (2006) Bilateral basal ganglia activation associated with sensorimotor adaptation. Exp Brain Res (in press)

Shadmehr R, Holcomb HH (1997) Neural correlates of motor memory consolidation. Science 277:821–825

Smith MA, Shadmehr R (2005) Intact ability to learn internal models of arm dynamics in Huntington's disease but not cerebellar degeneration. J Neurophysiol 93:2809–2821

Stoffers D, Berendse HW,Deijen JB, Wolters EC (2002) The influence of computer experience on visuo-motor control: implications for visuo-motor testing in Parkinson's disease. Neuropsychologica 40(11):1779–1785

Teulings HL, Contreras-Vidal JL, Stelmach GE, Adler CH (2002) Handwriting size adaptation under distorted visual feedback in Parkinson's disease patients, elderly controls and young controls. J Neurol Neurosurg and Psychiat 72:315–324